Short Communication

Evaluation of rice husk ash in adsorption of Remazol Red dye from aqueous media

José Arnaldo Santana Costa[1,2] · Caio Marcio Paranhos[2]

Abstract

The rice husk ash (RHA) extracted from the rice husk (RH) was measured on the removal of the Remazol Red dye. Adsorption variables such as solution pH, dye concentration, adsorbent amount, contact time, and reuse of the RHA were measured. The adsorption equilibrium was achieving in approximately 30 min, due to the rapid electrostatic attraction between the OH_2^+ groups of the RHA surface and the sulfonic groups of the dye, which occurred mainly at a pH = 2 value. The removal efficiency of the RHA decreased when the initial dye concentrations were higher, due to pore-filling within of the RHA structure with the migration dye molecules. However, the removal percentage increased with increasing adsorbent amount. The adsorption data were suitable with the Freundlich isotherm and pseudo-second order models.

Graphical abstract

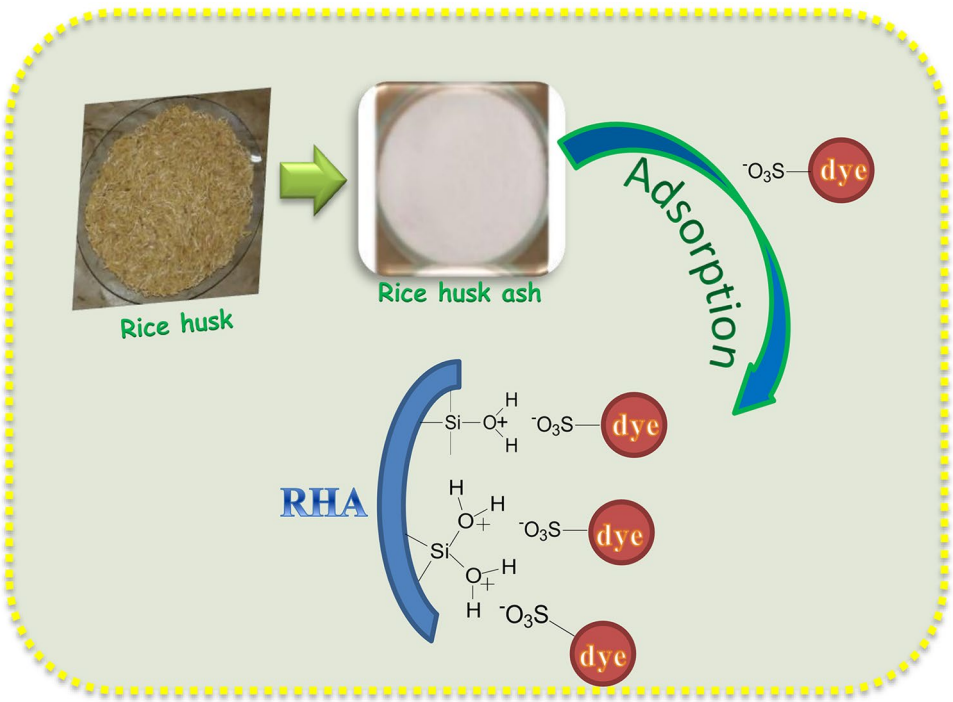

Preparation of the rice husk ash (RHA) and adsorption process of the Remazol Red dye by RHA.

✉ José Arnaldo Santana Costa, josearnaldo@ua.pt | [1]CICECO, Department of Chemistry, University of Aveiro, 3810-193 Aveiro, Portugal. [2]Polymer Laboratory, Department of Chemistry, Federal University of São Carlos, 13565-905 São Carlos, São Paulo, Brazil.

SN Applied Sciences (2019) 1:397 | https://doi.org/10.1007/s42452-019-0436-1

Received: 14 February 2019 / Accepted: 1 April 2019

Published online: 03 April 2019

Keywords Rice husk · Rice husk ash · Adsorption · Dye · Remazol red

1 Introduction

The production of waste from industrial activities is enormous, so the reduction of waste generation needs to be optimized; however this is a limited technology [1, 2]. Therefore, the recycling of these agroindustrial wastes is a plausible alternative to minimize their possible impacts on the environment [1, 3]. Rice is very consumed by the Brazilian population, since this cereal is among the highlights of the agricultural crops of this country [4]. The processing of the rice leads to the generation of the rice husk (RH) as the main residue, and this can represent about 20% of the production [5–7]. The production of the rice husk as a residue in Brazil was approximately 2.3 million tons in 2018, but the world production of the RH was much higher (around 154 million tons) [4].

The amorphous silica from RH may have its chemical purity and particle size modified by the thermal treatment temperature [8]. The rice husk ash (RHA) obtained from RH can be contains > 99% (w/w) silica and some amount of impurities [1, 9, 10], however, in order to obtain such a high silica content, the RH should be subjected to a water washing process in order to remove unwanted materials and then be pretreated with an acidic or basic solution, in order to remove impurities [1]. Thus, the RHA can be used as an alternative sorbent because the adsorption technology is an efficient and green process for the removal of different toxic and persistent pollutants present in the environment.

Disposal of untreated organic waste in the aquatic ecosystem is a global issue, mainly because these pollutants can cause serious damage to aquatic organisms as well as to humans [11, 12]. Among the main organic pollutants are dyes, which are classified as toxic and carcinogenic. However, despite its proven toxicity, synthetic dyes are still widely used in the textile industry [13].

Different methods of treatment of wastewaters with physical separation [14], chemical oxidation [15, 16], and biological degradation [17] have been reported in the removal of the dye. In view of the different methods for remediation of the dye, the adsorption has a great prominence due to its operational facilities and for being considered a green technology. Some studies found in the literature have reported the removal of dye from aqueous media using a variety of adsorbent materials. Huang et al. [18] employed modified bentonite for remove Rhodamine B and Acid Red 1, while Liu et al. [19] used mesoporous carbons on the adsorption of Acid Red 73 and Reactive Black 5. Zeolitic imidazolate framework was used by Li et al. [20] to remove Rhodamine B, Methyl Orange, and Methylene Blue.

In the literature, some studies report the removal of dye from the use of RHA as adsorbent material, for example, Sumanjit and Prasad [21] used the rice husk ash for the removal of the acid dyes, Lakshmi et al. [22] performed the adsorption tests of the carmine dye, Sharma et al. [23] removed the methylene blue from aqueous waste, and Bhowmick et al. [24] used the RHA for the removal of the *Amaranthus gangeticus* pigments as dye, while that Sethaya et al. [25] and Akshaya et al. [26] performed the removal of the methylene blue and reactive yellow dyes, respectively, on the other hand, Peres et al. [27] used a bio-nanosilica obtained from rice husk for the adsorption of crystal violet.

Thus, in this investigation, the RHA used for the adsorption of the Remazol Red dye was obtained from the optimization of the calcination time and temperature of the RH of the agulhinha variety from Brazil. In addition to the biogeographic importance of the RH used, we highlight the importance of the thermal treatment performed to obtain a rice husk ash with excellent structural and texture properties. On the other hand, up to the present moment we have not found any investigation that has used a Brazilian RHA to remove Remazol Red dye, in that way, the adsorption process was evaluated by means of kinetic and isotherms batch experiments.

2 Experimental

2.1 Collection of the RH and obtain of the RHA

The rice husk of the agulhinha (Indian origin) variety was given by the Brazilian Agricultural Research Corporation (Embrapa), São Carlos, São Paulo, Brazil. Thermal treatment performed to obtain RHA from RH and characterizations of the RH and RHA are reported previously [1].

2.2 Characterization of the RH and RHA

The characterization of the RH and RHA was complemented by scanning electron microscopy (SEM) analysis. SEM analysis was performed in a Phillips FEG-XL 30 microscopy in a secondary electron detector and with an accelerator power of 3 kV [28].

2.3 Batch adsorption experiments

A stock solution of 500 mg L^{-1} Remazol Red dye was prepared in distilled water. Stock solution of the dye

was dilute a posteriori to achieve specific concentrations when necessary. Tests to evaluate the effects of the pH, initial concentrations of the dye, adsorbent amount, contact time, and reuse were conducted in amber flasks at 25 °C, under mechanical agitation at 400 rpm. All the tests were performed in duplicate, using 0.10 g of the RHA and 10 mL of the solution of Remazol Red dye. After each set time, the samples were allowed to decant for 5 min and then filtered. The determination of the residual concentration after adsorption process was obtained in a Varian spectrophotometer (Cary 100) with the maximum absorbance of 520 nm of the Remazol Red, and finally the results were calculated and denoted in adsorbed amount and removal percentage of dye, according to Eqs. 1 and 2, respectively:

$$q_e = \frac{(C_0 - C_e)V}{m}, \quad (1)$$

$$\%\text{Removal} = \frac{(C_o - C_e)}{C_o} \times 100, \quad (2)$$

where q_e is the adsorbed amount of the Dye (mg g^{-1}), C_e and C_o are the equilibrium and initial concentrations of the dye (mg L^{-1}), respectively, m is the mass of the RHA (g), and V is the volume of the solution (L).

2.3.1 Effect of solution pH

The removal process of the dye by RHA was optimized at pH values in the range 2–12 to determine the ideal pH of the adsorption process. Solutions of 0.10 mol L^{-1} HCl or 0.10 mol L^{-1} NaOH were used for pH adjustments.

2.3.2 Effect of initial dye concentration

Concentrations of the dye in the range of 10–150 mg L^{-1} were used on the adsorption assays at a fixed pH value of 2 and with duration of 12 h.

2.3.3 Effect of sorbent amount

Values of the mass of the RHA in the range of 10–100 mg were used at a solution pH of 2, with time of 12 h, and concentration of 10 mg L^{-1} of dye.

2.3.4 Effect of contact time

Contact times in the range 0–300 min were studied using 100 mg of the RHA, solution pH equal to 2, and a concentration of 10 mg L^{-1}.

2.3.5 Regeneration of the RHA

At the end of the adsorption the saturated RHA was separated by filtration, and then regenerated by shaking in a solution of 0.1 mol L^{-1} NaOH, followed with centrifugation, washing, and drying at 70 °C. The regenerated RHA was reused in the next run under the same conditions.

3 Results and discussion

3.1 Characterization of the RH and the RHA

The characterizations of the RH and RHA are reported previously [1], the same were characterized by Fourier transform infrared spectroscopy (FTIR), X-ray fluorescence (XRF), thermogravimetric analysis (TGA), X-ray diffractometry (XRD), digital photographic images, and nitrogen adsorption–desorption isotherms. Thus, the FTIR and TGA results showed that the cellulose, hemicellulose, and lignin are the main components of the RH, as well as the silica bonded to these fibers, however the XRD analysis showed that RH has a crystalline structure. On the other hand, the presence of silica in RH was confirmed by the characterization performed in the RHA (A2-700), which presented a high SiO_2 content, an amorphous silica pattern, absence of organic matter, and high surface area (S_{BET} = 293.89 m^2 g^{-1}) and total pore volume (V_T = 0.36 cm^3 g^{-1}) according to with the XRF, XRD, digital photographic image, and N_2 adsorption results, respectively [1].

The SEM images obtained for untreated and treated RH and RHA are shown in Fig. 1. The untreated RH showed an external epidermis, which is well-organized and has a rippled surface with an elongated and contorted shape, as well as the appearance of a corn cob. However, after the acid treatment carried out therein (Fig. 1b), it is possible to observe that the surface of the RH has become more rough, due to the dilution or destruction of the amorphous region of the fibers present in the rice husk [1, 29]. Thus, it can be observed that Fig. 1c, which presents the external epidermis of the RHA, presents the same characteristic of the raw RH, however, in the external epidermis it concentrates the greater silica content [3, 30]. Therefore, Fig. 1d shows the internal epidermis of the RHA, which shows the porous structure known as the silica skeleton, from the burning of the organic matter of the RH fibers, and this region also contains a considerable silica amount [31, 32].

3.2 Batch adsorption experiments

3.2.1 Effect of solution pH

The variation of solution pH in an adsorption process is a very important parameter, since this variation can alter the degree of ionization of the molecules that will be adsorbed, as well as the surface of the adsorbent material, in this case the RHA. Thus, this variation can directly reflect in the adsorption efficiency of the RHA in remediation of Red Remazol [33]. Figure 2 shows adjust of pH in the removal of Remazol Red by RHA.

As shown in Fig. 2, it can be seen that the decrease in pH value caused an increase in adsorption efficiency of the RHA. This increase can be attributed by protonation of O–H groups present in the pores of the RHA, as well as the anionic properties of the Remazol Red dye. Therefore, the adsorption of dye by RHA is attributed to the electrostatic attraction between the OH_2^+ groups and the sulfonic groups of the dye at the adsorbent/adsorbate interface [13]. On the other hand, at pH > 7, there is a large amount of OH^- ions that promote the deprotonation of the O–H groups, and thus, these OH^- ions compete and/or interact with the dye molecules on the active sites of RHA, thereby providing a reduction of the adsorption efficiency of the RHA. So, the other experiments were performed at pH 2.

3.2.2 Effect of initial dye concentration

Figure 3 shows the results obtained on the adsorption process of the Remazol Red by the RHA from the variation of the adsorbate concentration. It is possible to observe that the removal percentage value of the Remazol Red adsorbed decreased when the initial concentrations were higher. This behavior can be related to the increase in the number of the Remazol Red molecules competing for the adsorption sites in the pores of the RHA [13], as well as the saturation of the adsorption sites of the RHA, due to pore-filling within of the RHA with migration towards sites deeper of the voluminous molecules of the Remazol Red dye [34].

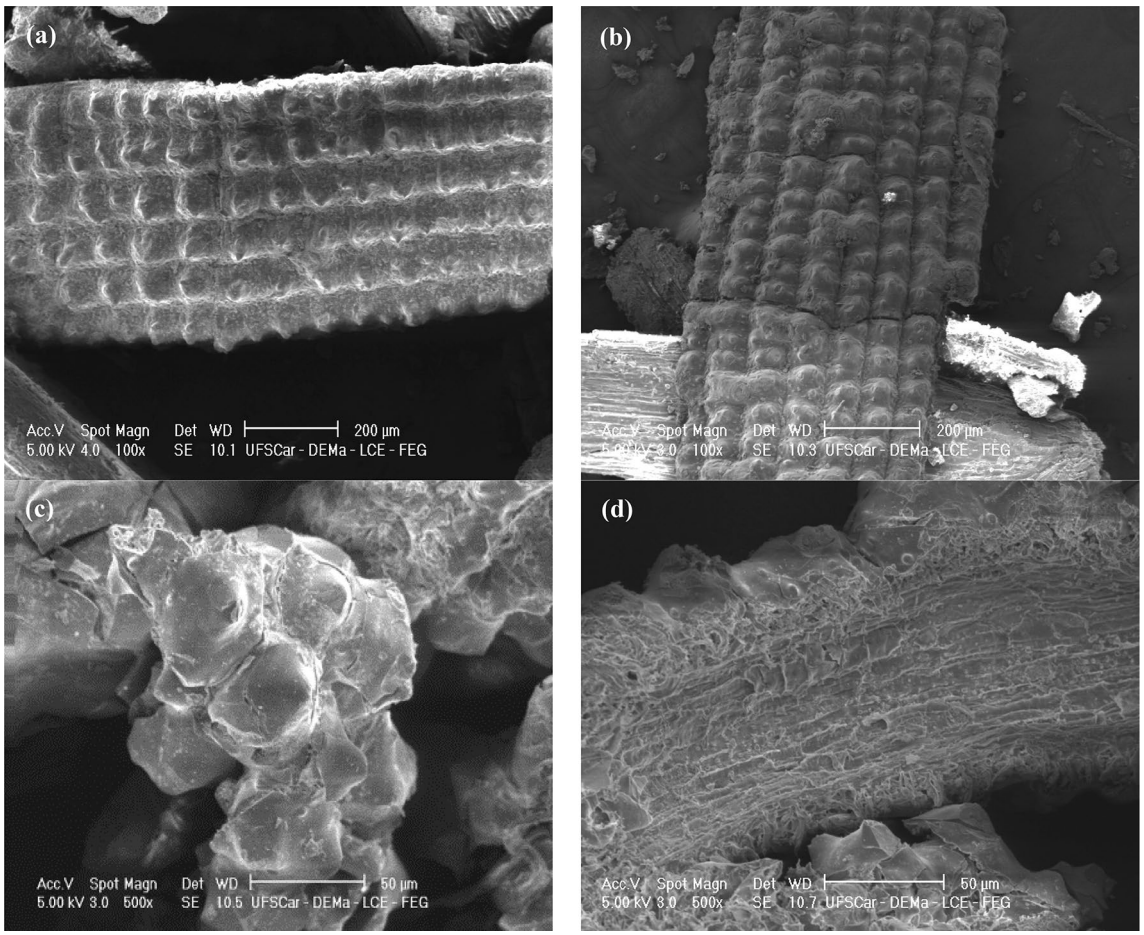

Fig. 1 Scanning electron micrograph of the **a** untreated and **b** treated RH, **c** untreated and **d** treated RHA

3.2.3 Effect of sorbent amount

Figure 4 shows influence of the sorbent amount in the adsorption process of the Remazol Red by RHA. Thus, it is possible to observe that the increase of the RHA mass caused an increase of the adsorption efficiency of the Remazol Red, according to Fig. 4. This same behavior was seen by Santos et al. [13], which can be attributed there is a wide surface area available for adsorption of the dye, this behavior was observed due to the excellent values of the BET surface area, pore volume and diameter, and average pore size presented by RHA [1]. The adsorption dosage of 100 mg was used for the further studies to evaluate the effect of the others parameters.

3.2.4 Effect of contact time

Figure 5 shows the results obtained of the removal of the Remazol Red by the RHA as a function of the adsorption time. It is possible to observe that after the initial 30 min the adsorption process reached equilibrium, with the maximum removal percentage value of 86.40%. Thus, according to our previous work [34], this adsorption process is governed by two kinetic stages, the first with a fast interaction in the initial minutes and the second process, much slower, until to adsorption equilibrium. The results indicated that the main interaction mechanism can be related to rapid electrostatic attraction between the OH_2^+ groups of the RHA surface and the sulfonic groups of the dye, immediately after exposure, corroborating with the results obtained in the effects of the solution pH and RHA amount. Therefore, it can be concluded that a large pore volume of the RHA was favorable for adsorption performance.

3.3 Kinetics of adsorption

The adsorption process can be better evaluated by comparing the experimental data with the theoretical adsorption models [34]. Thus, the pseudo–first order and pseudo–second order kinetic models have been used according to the methodology described in our previous works [34, 35]. Table 1 shows the adsorption kinetic parameters obtained from the experimental data on the adsorption of the Remazol Red dye by RHA, these parameters were obtained using the pseudo-first order and pseudo-second order kinetic models. As shown in Table 1, the linear correlation coefficient (r^2) value was higher for the data obtained from the pseudo-second order model than the pseudo-first order model, showing that there an adjustment of the experimental data with the pseudo-second order model. Thus, the quantity adsorbed measured experimentally ($q_{e(exp.)}$) value is very close to the $q_{e(cal.)}$ value obtained from the pseudo-second order model, showing the adequacy of the experimental data to this model [34, 36]. In addition, the k_2 and h_i values obtained with the pseudo-second order model were higher than the k_1 and h_i values calculated from pseudo-first order model, providing further confirmation of the fit of the experimental data to pseudo-second order model.

3.4 Adsorption isotherms

According to Santos et al. [13] the Freundlich and Langmuir models can predict the behavior of adsorbate at the

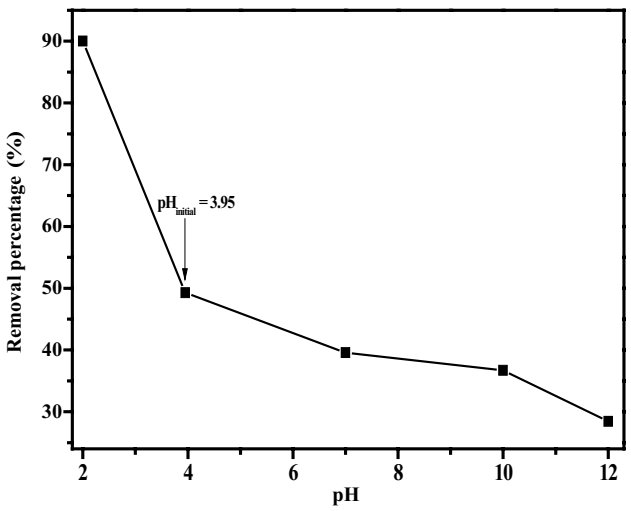

Fig. 2 Effect of the solution pH on the removal percentage of Remazol Red dye

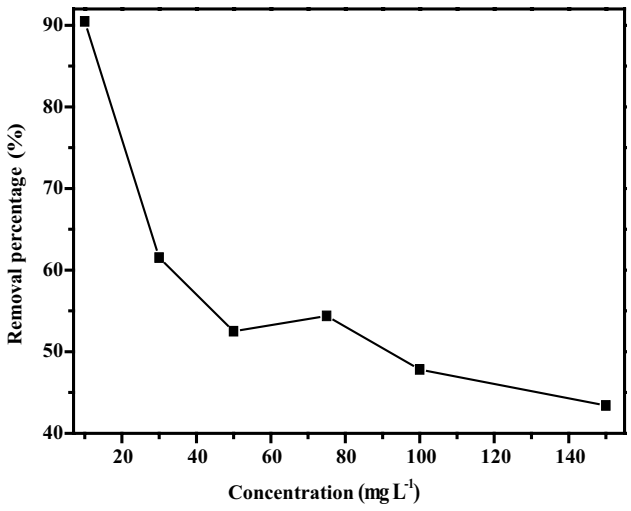

Fig. 3 Effect of the initial dye concentration on the removal percentage of Remazol Red dye

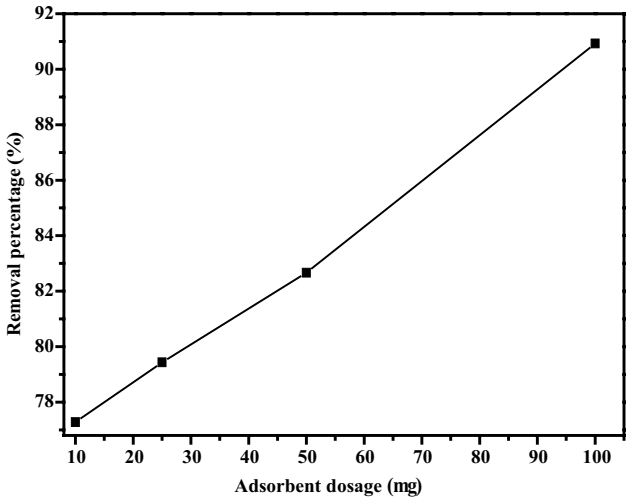

Fig. 4 Effect of the sorbent amount on the removal percentage of Remazol Red dye

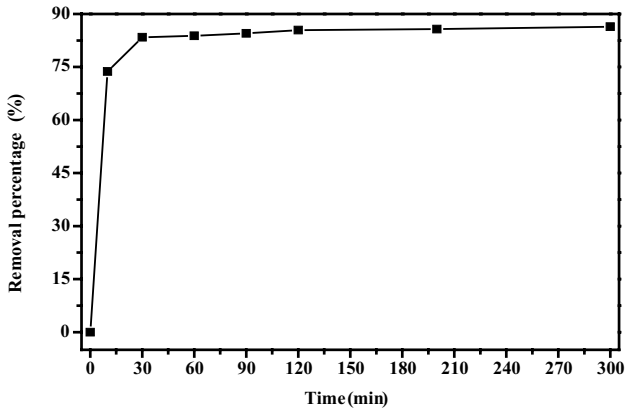

Fig. 5 Effect of the contact time on the removal percentage of Remazol Red dye

solid/liquid interface in the adsorption process. Adsorption data have been used according to the methodology described our previous works [34, 35]. Figure 6 shows the adsorption isotherms of experimental data of adsorption of the Remazol Red by RHA, as well as of Freundlich and Langmuir models. The adsorption capacity (K_F) and

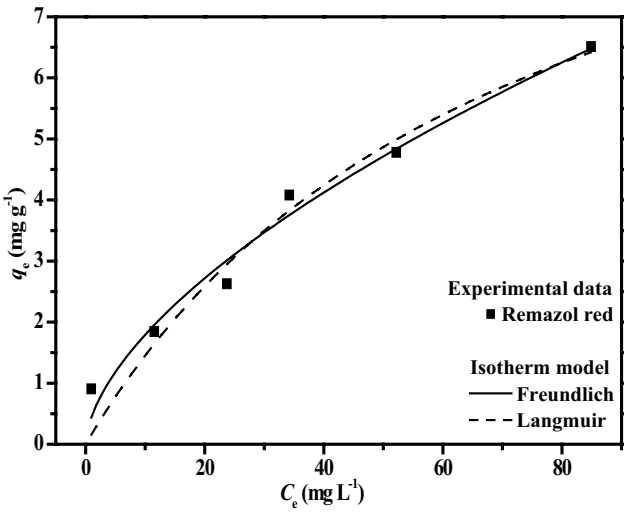

Fig. 6 Comparison of equilibrium data obtained using the Freundlich and Langmuir isotherm models applied on the removal of the Remazol Red dye by RHA

intensity (n), maximum adsorption capacity (Q_{max}), Langmuir constant (b), and linear correlation coefficient (r^2) values obtained for the two models are given in Table 2.

As can be seen in Table 2, the Freundlich model is more representative than Langmuir model for the experimental data of equilibrium adsorption of the Remazol Red by the RHA, according to the r^2 values obtained by the two models. According to Santos et al. [13] the $n > 1$ value for the removal of the dye is an indicative of the positive cooperation between Remazol Red molecules, so the removal process is not restricted to the formation of the monolayer, as well as the system has a heterogeneous active site energy distribution and a possible interaction between the adsorbed molecules of the Remazol Red dye within of the pores of the RHA. In addition, this result can be due to the textural and structural properties of the RHA promoting the diffusion and transport of the dye molecules onto the adsorbent.

3.5 Regeneration of the adsorbent

The reuse of an adsorbent material is a very important characteristic, mainly from the economic point

Table 1 Comparison of the pseudo-first order and pseudo-second order kinetic models on the removal of the Remazol Red dye by RHA

Remazol red	$q_{e\ (exp.)}$ (mg g^{-1})	Pseudo–first order				Pseudo–second order			
		$q_{e\ (calc.)}$ (mg g^{-1})	k_1 (min^{-1})	h_i [(mg g^{-1})^2 min^{-1}]	r^2	$q_{e\ (calc.)}$ (mg g^{-1})	k_2 (g mg^{-1} min^{-1})	h_i (mg g^{-1} min^{-1})	r^2
	0.86	0.85	0.20	0.14	0.998	0.87	0.68	0.51	0.999

$q_{e\ (exp.)}$ and $q_{e\ (calc.)}$: quantities of Remazol red dye adsorbed at equilibrium, obtained experimentally and calculated, respectively; k_1 and k_2: pseudo-first order and pseudo-second order rate constants, respectively; r^2: linear correlation coefficient; h_i: initial adsorption

Table 2 Comparison of equilibrium data obtained using the Freundlich and Langmuir isotherm models applied on the removal of the Remazol Red dye by RHA

Remazol red	Freundlich			Langmuir		
	K_F (L g^{-1})	n	r_F^2	Q_{max} (mg g^{-1})	b (L mg^{-1})	r_L^2
	0.45	1.66	0.971	11.83	0.014	0.952

K_F: adsorption capacity; n: adsorption intensity; r^2: linear correlation coefficient; Q_{max}: maximum adsorption capacity, and b: Langmuir constant

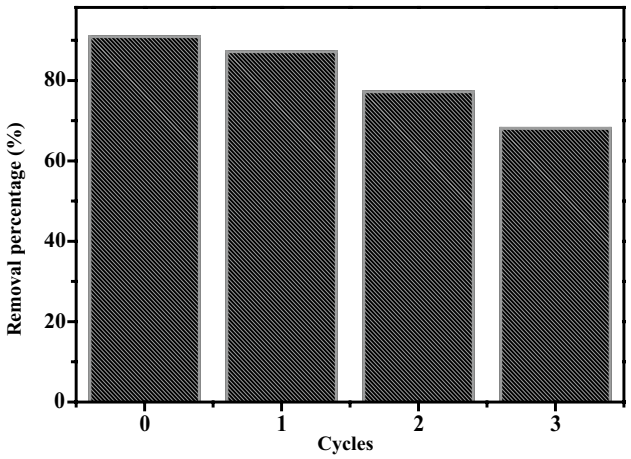

Fig. 7 Reuse cycles of RHA on the removal percentage of Remazol Red dye

of view, since these can be regenerated and reused in other adsorption processes. Figure 7 shows the results obtained from the reuse cycles of RHA on the removal of the Remazol Red. The adsorption efficiency of the RHA slightly decreased with increasing number of cycles. It was observed that the adsorption efficiency values decreased from 90.93 to 68.07% after 3 cycles of reuse, indicating that the RHA could be effectively used as a reusable adsorbent in the removal of the Remazol Red dye.

4 Conclusions

The adsorption equilibrium of the Remazol Red dye by RHA was achieving in approximately 30 min. A higher sorbent amount, as well as low pH medium favored the adsorption process, however, the adsorption efficiency of the RHA decreased with increase of the initial dye concentration. The pseudo-second order and Freundlich models are more representative than the pseudo-first order and Langmuir models for the kinetics and equilibrium experimental data of adsorption of the Remazol Red by the RHA, respectively. The adsorption results obtained suggested that the RHA is a strong candidate as an adsorbent material for the removal of dyes from textile industry wastewater.

Acknowledgements The authors thank FAPESP (Research Support Foundation of the State of São Paulo) (Grants 2014/05679-4, 2017/06775-5, and 2018/18894-1), CAPES (Coordination for the Improvement of Higher Education Personnel) (Grant 309342/2010-4), and CDMF (Center for the Development of Functional Materials) (Grant 2013/07296-2) for the financial support.

Compliance with ethical standards

Conflict of interest The authors declare that they have no conflict of interest.

References

1. Costa JAS, Paranhos CM (2018) Systematic evaluation of amorphous silica production from rice husk ashes. J Clean Prod 192:688–697. https://doi.org/10.1016/j.jclepro.2018.05.028
2. Santos LFS, de Jesus RA, Costa JAS et al (2019) Evaluation of MCM-41 and MCM-48 mesoporous materials as sorbents in matrix solid phase dispersion method for the determination of pesticides in soursop fruit (*Annona muricata*). Inorg Chem Commun 101:45–51. https://doi.org/10.1016/j.inoche.2019.01.013
3. Della VP, Kühn I, Hotza D (2005) Reciclagem de Resíduos Agro-Industriais: cinza de Casca de Arroz como Fonte Alternativa de Sílica. Cerâm Ind 10:22–25
4. FAO (2018) Production international trade domestic prices. Rice Market Monitor 21:1–35
5. An D, Guo Y, Zhu Y, Wang Z (2010) A green route to preparation of silica powders with rice husk ash and waste gas. Chem Eng J 162:509–514. https://doi.org/10.1016/j.cej.2010.05.052
6. Ng YC, Jei CY, Shamsuddin M (2009) Titanosilicate ETS-10 derived from rice husk ash. Microporous Mesoporous Mater 122:195–200. https://doi.org/10.1016/j.micromeso.2009.03.001
7. Ng EP, Awala H, Tan KH et al (2015) EMT-type zeolite nanocrystals synthesized from rice husk. Microporous Mesoporous Mater 204:204–209. https://doi.org/10.1016/j.micromeso.2014.11.017
8. Ali IO, Hassan AM, Shaaban SM, Soliman KS (2011) Synthesis and characterization of ZSM-5 zeolite from rice husk ash and their adsorption of Pb2 + onto unmodified and surfactant-modified zeolite. Sep Purif Technol 83:38–44. https://doi.org/10.1016/j.seppur.2011.08.034
9. Panpa W, Jinawath S (2009) Synthesis of ZSM-5 zeolite and silicalite from rice husk ash. Appl Catal B 90:389–394. https://doi.org/10.1016/j.apcatb.2009.03.029
10. Muniandy L, Adam F, Mohamed AR, Ng EP (2014) The synthesis and characterization of high purity mixed microporous/mesoporous activated carbon from rice husk using chemical activation with NaOH and KOH. Microporous Mesoporous Mater 197:316–323. https://doi.org/10.1016/j.micromeso.2014.06.020
11. Chen M, Bao C, Cun T, Huang Q (2017) One-pot synthesis of ZnO/oligoaniline nanocomposites with improved removal of organic

dyes in water: effect of adsorption on photocatalytic degradation. Mater Res Bull 95:459–467. https://doi.org/10.1016/j.materresbull.2017.08.017
12. Oveisi M, Asli MA, Mahmoodi NM (2018) MIL-Ti metal-organic frameworks (MOFs) nanomaterials as superior adsorbents: synthesis and ultrasound-aided dye adsorption from multicomponent wastewater systems. J Hazard Mater 347:123–140. https://doi.org/10.1016/j.jhazmat.2017.12.057
13. Santos DO, Santos MLN, Costa JAS et al (2013) Investigating the potential of functionalized MCM-41 on adsorption of Remazol Red dye. Environ Sci Pollut Res 20:5028–5035. https://doi.org/10.1007/s11356-012-1346-6
14. Wan Z, Li D, Jiao Y et al (2017) Bifunctional MoS2coated melamine-formaldehyde sponges for efficient oil–water separation and water-soluble dye removal. Appl Mater Today 9:551–559. https://doi.org/10.1016/j.apmt.2017.09.013
15. Bassyouni DG, Hamad HA, El-Ashtoukhy ESZ et al (2017) Comparative performance of anodic oxidation and electrocoagulation as clean processes for electrocatalytic degradation of diazo dye Acid Brown 14 in aqueous medium. J Hazard Mater 335:178–187. https://doi.org/10.1016/j.jhazmat.2017.04.045
16. Rajoriya S, Bargole S, George S, Saharan VK (2018) Treatment of textile dyeing industry effluent using hydrodynamic cavitation in combination with advanced oxidation reagents. J Hazard Mater 344:1109–1115. https://doi.org/10.1016/j.jhazmat.2017.12.005
17. Sun S, Xie S, Chen H et al (2016) Genomic and molecular mechanisms for efficient biodegradation of aromatic dye. J Hazard Mater 302:286–295. https://doi.org/10.1016/j.jhazmat.2015.09.071
18. Huang Z, Li Y, Chen W et al (2017) Modified bentonite adsorption of organic pollutants of dye wastewater. Mater Chem Phys 202:266–276. https://doi.org/10.1016/j.matchemphys.2017.09.028
19. Liu F, Guo Z, Ling H et al (2016) Effect of pore structure on the adsorption of aqueous dyes to ordered mesoporous carbons. Microporous Mesoporous Mater 227:104–111. https://doi.org/10.1016/j.micromeso.2016.02.051
20. Li Y, Zhou K, He M, Yao J (2016) Synthesis of ZIF-8 and ZIF-67 using mixed-base and their dye adsorption. Microporous Mesoporous Mater 234:287–292. https://doi.org/10.1016/j.micromeso.2016.07.039
21. Sumanjit Prasad N (2001) Adsorption of dyes on Rice Husk Ash. Indian J Chem 40:388–391
22. Lakshmi UR, Srivastava VC, Mall ID, Lataye DH (2009) Rice husk ash as an effective adsorbent: evaluation of adsorptive characteristics for Indigo Carmine dye. J Environ Manage 90:710–720. https://doi.org/10.1016/j.jenvman.2008.01.002
23. Sharma P, Kaur R, Baskar C, Chung WJ (2010) Removal of methylene blue from aqueous waste using rice husk and rice husk ash. Desalination 259:249–257. https://doi.org/10.1016/j.desal.2010.03.044
24. Bhowmick AC, Rahaman MA, Islam M et al (2015) Comparative adsorption study on rice husk and rice husk ash by using amaranthus gangeticus pigments as dye. Eur Sci J 11:1857–7881
25. Setthaya N, Chindaprasirt P, Yin S, Pimraksa K (2017) TiO_2-zeolite photocatalysts made of metakaolin and rice husk ash for removal of methylene blue dye. Powder Technol 313:417–426. https://doi.org/10.1016/j.powtec.2017.01.014
26. Akshaya A, Chinnaiyan P, Unni D, Keerthana G (2018) Use of TiO_2 and rice husk ash to study the removal of reactive yellow dye as contaminant in water. Mater Today Proc 5:24268–24276. https://doi.org/10.1016/j.matpr.2018.10.222
27. Peres EC, Favarin N, Slaviero J et al (2018) Bio-nanosilica obtained from rice husk using ultrasound and its potential for dye removal. Mater Lett 231:72–75. https://doi.org/10.1016/j.matlet.2018.08.018
28. Costa JAS, Vedovello P, Paranhos CM (2019) Use of ionic liquid as template for hydrothermal synthesis of the MCM-41 mesoporous material. Silicon. https://doi.org/10.1007/s12633-019-00121-9
29. Johara N, Ahmada I, Dufresne A (2012) Extraction, preparation and characterization of cellulose fibres and nanocrystals from rice husk. Ind Crops Prod 37:93–99. https://doi.org/10.1016/j.indcrop.2011.12.016
30. Della V, Kuhn I, Hotza D (2002) Rice husk ash as an elemente source for active silicaproduction. Mater Lett 57:818–821. https://doi.org/10.1016/S0167-577X(02)00879-0
31. Ahmed AE, Adam F (2007) Indium incorporated silica from rice husk and its catalytic activity. Microporous Mesoporous Mater 103:284–295. https://doi.org/10.1016/j.micromeso.2007.01.055
32. Liou TH (2004) Preparation and characterization of nano-structured silica from rice husk. Mater Sci Eng A 364:313–323. https://doi.org/10.1016/j.msea.2003.08.045
33. Hu Y, He Y, Wang X, Wei C (2014) Efficient adsorption of phenanthrene by simply synthesized hydrophobic MCM-41 molecular sieves. Appl Surf Sci 311:825–830. https://doi.org/10.1016/j.apsusc.2014.05.173
34. Costa JAS, de Jesus RA, da Silva CMP, Romão LPC (2017) Efficient adsorption of a mixture of polycyclic aromatic hydrocarbons (PAHs) by Si–MCM–41 mesoporous molecular sieve. Powder Technol 308:434–441. https://doi.org/10.1016/j.powtec.2016.12.035
35. Costa JAS, Garcia ACFS, Santos DO et al (2015) Applications of inorganic-organic mesoporous materials constructed by self-assembly processes for removal of benzo[k]fluoranthene and benzo[b]fluoranthene. J Sol-Gel Sci Technol 75:495–507. https://doi.org/10.1007/s10971-015-3720-6
36. Costa JAS, Garcia ACFS, Santos DO et al (2014) A new functionalized MCM-41 mesoporous material for use in environmental applications. J Braz Chem Soc 25:197–207. https://doi.org/10.5935/0103-5053.20130284